Theoretical study of ^{3}He$(\mu^-, \nu_\mu)^3$H capture

L. E. Marcucci,[1,2] R. Schiavilla,[3,4] S. Rosati,[1,2] A. Kievsky,[2,1] and M. Viviani[2,1]

[1]*Department of Physics, University of Pisa, I-56100 Pisa, Italy*
[2]*INFN, Sezione di Pisa, I-56100 Pisa, Italy*
[3]*Department of Physics, Old Dominion University, Norfolk, Virginia 23529*
[4]*Jefferson Lab, Newport News, Virginia 23606*

The ^{3}He$(\mu^-, \nu_\mu)^3$H weak capture is studied using correlated-hyperspherical-harmonics wave functions, obtained from realistic Hamiltonians consisting of the Argonne v_{14} or Argonne v_{18} two-nucleon, and Tucson-Melbourne or Urbana-IX three-nucleon interactions. The nuclear weak charge and current operators have vector and axial-vector components with one- and two-body contributions. The axial-vector current includes the nucleon and Δ induced pseudoscalar terms, with coupling constants g_{PS} and g_{PS}^* derived from pion-pole dominance and partially conserved-axial-current hypothesis. The strength of the leading two-body operator is adjusted to reproduce the Gamow-Teller matrix element in tritium β decay. The calculated total capture rate is within $\sim 0.5\%$ of the most recent measurement, 1496 ± 4 sec^{-1}. The predictions for the capture rate and angular correlation parameters A_v, A_t, and A_Δ are found to be only very weakly dependent on the model input Hamiltonian. The variation of the observables with g_{PS} and g_{PS}^* and the theoretical uncertainties deriving from the model-dependent procedure used to constrain the axial current are investigated.

I. INTRODUCTION

The μ^- weak capture on ^{3}He can occur through three different hadronic channels:

$$\mu^- + {}^3\text{He} \rightarrow {}^3\text{H} + \nu_\mu \quad (70\%), \tag{1.1}$$

$$\mu^- + {}^3\text{He} \rightarrow n + d + \nu_\mu \quad (20\%), \tag{1.2}$$

$$\mu^- + {}^3\text{He} \rightarrow n + n + p + \nu_\mu \quad (10\%). \tag{1.3}$$

The focus of the present work is on the first process. Some of the nuclear physics issues in muon capture have been reviewed recently in Ref. [1].

The reaction (1.1) has been extensively studied through the years, both experimentally and theoretically. Measurements of the total capture rate have been performed since the early 1960s [2–4] up to until recently. The latest very precise experimental determination of this observable [5], 1496 ± 4 sec^{-1}, is consistent with the earlier measurements, the latter having considerably larger uncertainties, however.

Theoretical studies of reaction (1.1) have been carried out within two different frameworks: the so-called "elementary particle method" (EPM) and the fully microscopic approach. The EPM, first developed by Kim and Primakoff [6], is essentially a phenomenological approach, which parametrizes the nuclear (charge-changing) weak current in terms of the trinucleon form factors, in analogy to the nucleon weak current, and then attempts to derive these from other experiments. Within the EPM, it was shown in Ref. [7] that, if the hyperfine structure of the μ^- ^{3}He system is taken into account and the direction of the recoiling triton can be detected, there are, in addition to the capture rate, other observables, i.e., angular correlation parameters, which are more sensitive than the capture rate itself to the value of the nucleon pseudoscalar axial coupling constant g_{PS}. Indeed,

the possibility of determining g_{PS} from measurements of muon capture observables is one of the motivations for the interest that this process has generated over the years. Recently, one attempt has been made to measure the angular correlation parameter A_v [8], though the experimental result, which to our knowledge represents the first significant measurement of this observable, is affected by large systematic uncertainties. Therefore a comparison between theory and experiment will not be particularly meaningful for A_v. Experimental results with an improved accuracy are highly desirable.

In contrast, the fully microscopic approach is based on: (i) ^{3}H and ^{3}He wave functions as accurate as possible, to reduce uncertainties related to nuclear structure; (ii) a realistic model for the nuclear weak current and charge operators. The first microscopic calculation of reaction (1.1) was performed by Peterson in 1968 [9], and was reconsidered and improved by Phillips and collaborators in 1974 [10]. These studies, however, used nuclear wave functions which were approximate, and retained in the nuclear weak transition operators only single-nucleon terms, the impulse approximation (IA).

In the early 1990s, the muon capture on ^{3}He, including the total rate and angular correlation parameters mentioned above, have been extensively investigated, within the fully microscopic framework, by Congleton and Fearing [11], and Congleton and Truhlìk [12]. The most significant improvements in these studies, relative to those of the late 1960s [9] and early 1970s [10], are in the more accurate treatment of the trinucleon wave functions and of the weak interaction. The nuclear wave functions have been obtained from a realistic Hamiltonian based on the Argonne v_{14} two-nucleon [13] and Tucson-Melbourne three-nucleon [14] interactions, using the rearrangement coupled-channel method [15].

The study in Ref. [11] used the IA form of the nuclear weak current, and emphasized the need to go beyond single-

nucleon contributions for a realistic description of the process. This next step was carried out in Ref. [12], where a model for two-body components in the nuclear weak current was explicitly constructed. The calculated capture rate is in good agreement with the measured value, although the theoretical prediction suffers from a 2% uncertainty, which is rather large compared to the experimental error, and mostly arises from poor knowledge of some of the coupling constants and cutoff parameters entering the axial current.

The present work sharpens and updates that of Ref. [12]. Improvements in the modeling of two- and three-nucleon interactions and the nuclear weak current make the re-examination of process (1.1) especially timely. The initial and final state wave functions have been obtained, using the correlated-hyperspherical-harmonics method, from a nuclear Hamiltonian which consists of the Argonne v_{18} two-nucleon [16] and Urbana-IX three-nucleon [17] interactions. To make contact with the study of Ref. [12], however, and to have some estimate of the model dependence of the results, the older Argonne v_{14} two-nucleon and Tucson-Melbourne three-nucleon interaction models have also been used. Both these Hamiltonians reproduce the experimental binding energies and charge radii of the trinucleon systems.

The model for the nuclear weak current used in the present work has been developed in Refs. [18–20]. However, two additional contributions have been included: the one-body term associated with the induced pseudoscalar charge operator of the nucleon, and the induced pseudoscalar two-body term in the $N\Delta$-transition axial current. Both contributions are of order $O(q^2/m^2)$, where q is the momentum transfer in the process and m is the nucleon mass. They were neglected in the proton weak capture reactions studied in Refs. [18–20], for which $q \ll m$. A brief description of these operators is given in Sec. III.

Some of the differences between the model for the nuclear weak current of Ref. [12] and that adopted here should be noted. It is well known by now that the axial current associated with Δ excitation is the dominant (axial) two-body mechanism. In the present work, its strength, i.e., the $N\Delta$-transition axial coupling constant g_A^*, has been determined by fitting the measured Gamow-Teller matrix element in tritium β decay. The inherent model dependence of this procedure has been shown to be very weak in studies of the proton weak captures on ^{1}H [18] and ^{3}He [20]. In Ref. [18] predictions for the ^{1}H$(p,e^+\nu_e)^2$H cross section, obtained with a variety of modern high-quality two-nucleon interactions, differed by significantly less than 1%, once the coupling constant g_A^* had been fixed as described above within each given model Hamiltonian (for further discussion of this point as well as of the reasons for such a weak model dependence, see Ref. [18]). In Ref. [12], on the other hand, g_A^* is related to the $\pi N\Delta$ coupling constant $f_{\pi N\Delta}$, and values ranging from the quark-model to the Skyrme-soliton model predictions are used for $f_{\pi N\Delta}$.

There are additional differences in the detailed form of the pion range operators, which in Ref. [12] were derived from a phenomenological chiral Lagrangian containing contributions from π- and A_1-pole mediated currents. Congleton and

Truhlìk, though, ignored ρ-meson contributions both in the axial-vector and vector sectors of the weak current. These are retained in the present work. However, as it is clear from Ref. [12] and also from Sec. IV below, these differences have little numerical impact on the calculated muon capture observables.

Finally, the induced pseudoscalar term in the Δ axial current is ignored in Ref. [12], while here it is determined using pion-pole dominance and the partially conserved-axial-current (PCAC) hypothesis. The induced pseudoscalar coupling constant g_{PS}^* is related to g_A^* via the (extended) Goldberger-Treiman relation [21].

A crucial issue, though, remains to be addressed, namely the extent to which the present model for the nuclear weak current is successful in predicting observed weak transitions (note that the cross sections of the proton weak capture processes mentioned above are not known experimentally). The present work fulfils this need by showing that the calculated rate for μ^- capture on ^{3}He is in excellent agreement with the measured value.

This manuscript falls into five sections. In Sec. II explicit expressions for the rate and angular correlation parameters are derived in terms of reduced matrix elements of multipole operators, while in Sec. III the model for the weak current is succintly described. The results are presented and discussed in Sec. IV, and some concluding remarks are given in Sec. V.

II. OBSERVABLES

The muon capture on ^{3}He is induced by the weak interaction Hamiltonian [22,23]

$$H_W = \frac{G_V}{\sqrt{2}} \int d\mathbf{x}\, l_\sigma(\mathbf{x}) j^\sigma(\mathbf{x}), \qquad (2.1)$$

where G_V is the Fermi coupling constant, $G_V = 1.149\,39 \times 10^{-5}$ GeV^{-2} [24], and l_σ and j^σ are the leptonic and hadronic current densities, respectively. The former is given by

$$l_\sigma(\mathbf{x}) = e^{-i\mathbf{k}_\nu \cdot \mathbf{x}}\, \bar{u}(\mathbf{k}_\nu, h_\nu)\gamma_\sigma(1-\gamma_5)\psi_\mu(\mathbf{x}, s_\mu), \quad (2.2)$$

where $\psi_\mu(\mathbf{x}, s_\mu)$ is the ground-state wave function of the muon in the Coulomb field of the ^{3}He nucleus, and $u(\mathbf{k}_\nu, h_\nu)$ is the spinor of a muon neutrino with momentum $\mathbf{k}_\nu$, energy E_ν ($=k_\nu$), and helicity h_ν. While in principle the relativistic solution of the Dirac equation could be used, in practice it suffices to approximate

$$\psi_\mu(\mathbf{x}, s_\mu) \simeq \psi_{1s}(x)\chi(s_\mu) \equiv \psi_{1s}(x)u(\mathbf{k}_\mu, s_\mu) \quad \mathbf{k}_\mu \to 0, \qquad (2.3)$$

since the muon velocity $v_\mu \simeq Z\alpha \ll 1$ (α is the fine-structure constant and $Z=2$). Here $\psi_{1s}(x)$ is the $1s$ solution of the Schrödinger equation and, since the muon is essentially at rest, it is justified to replace the two-component spin state $\chi(s_\mu)$ with the four-component spinor $u(\mathbf{k}_\mu, s_\mu)$ in the limit $\mathbf{k}_\mu \to 0$. This will allow us to use standard techniques to carry out the spin sum over s_μ at a later stage.

In order to account for the hyperfine structure in the initial system, the muon and ^{3}He spins are coupled to states with total spin f equal to 0 or 1. The transition amplitude can then be conveniently written as

$$T_W(f, f_z; s_3', h_\nu) \equiv \langle {}^3\mathrm{H}, s_3'; \nu, h_\nu | H_W | (\mu, {}^3\mathrm{He}); f, f_z \rangle$$

$$\simeq \frac{G_V}{\sqrt{2}} \psi_{1s}^{\mathrm{av}} \sum_{s_\mu, s_3} \left\langle \frac{1}{2} s_\mu, \frac{1}{2} s_3 \middle| f, f_z \right\rangle l_\sigma(h_\nu, s_\mu)$$

$$\times \langle {}^3\mathrm{H}, s_3' | j^\sigma(\mathbf{q}) | {}^3\mathrm{He}, s_3 \rangle, \qquad (2.4)$$

where

$$l_\sigma(h_\nu, s_\mu) \equiv \bar{u}(\mathbf{k}_\nu, h_\nu) \gamma_\sigma(1 - \gamma_5) u(\mathbf{k}_\mu, s_\mu), \qquad (2.5)$$

and the Fourier transform of the nuclear weak current has been introduced as

$$j^\sigma(\mathbf{q}) = \int d\mathbf{x} \, e^{i\mathbf{q} \cdot \mathbf{x}} j^\sigma(\mathbf{x}) \equiv (\rho(\mathbf{q}), \mathbf{j}(\mathbf{q})), \qquad (2.6)$$

with the leptonic momentum transfer $\mathbf{q}$ defined as $\mathbf{q} = \mathbf{k}_\mu - \mathbf{k}_\nu \simeq -\mathbf{k}_\nu$. The Bohr radius of the muonic atom in the ground state is about 130 fm, i.e., much larger than the nuclear radius, and it is therefore well justified to factor out $\psi_{1s}(x)$ from the matrix element of $j^\sigma(\mathbf{q})$ between the trinucleon ground states, by approximating it as [22,23]

$$|\psi_{1s}^{\mathrm{av}}|^2 \equiv \mathcal{R} |\psi_{1s}(0)|^2 = \mathcal{R} \frac{(2\alpha m_r)^3}{\pi}, \qquad (2.7)$$

where $\psi_{1s}(0)$ denotes the Bohr wave function evaluated at the origin for a point charge $2e$, m_r is the reduced mass of the $\mu^- \, {}^3$He system, and the factor $\mathcal{R}$ approximately accounts for the finite extent of the nuclear charge distribution [22,23]. The value $\mathcal{R} = 0.98$ is used here [11].

Standard techniques [20,23] are now used to carry out the multipole expansion of the weak charge $[\rho(\mathbf{q})]$ and current $[\mathbf{j}(\mathbf{q})]$ operators in the general case in which θ is the angle between the spin quantization axis (the $\hat{\mathbf{z}}$ axis) and the leptonic momentum transfer $\mathbf{q}$:

$$\langle {}^3\mathrm{H}, s_3' | \rho(\mathbf{q}) | {}^3\mathrm{He}, s_3 \rangle = \sqrt{2\pi} \sum_{l=0,1} \sqrt{2l+1} \, i^l d_{m,0}^l(-\theta)$$

$$\times \left\langle \frac{1}{2} s_3, lm \middle| \frac{1}{2} s_3' \right\rangle C_l(q), \qquad (2.8)$$

$$\langle {}^3\mathrm{H}, s_3' | j_z(\mathbf{q}) | {}^3\mathrm{He}, s_3 \rangle = -\sqrt{2\pi} \sum_{l=0,1} \sqrt{2l+1} \, i^l d_{m,0}^l(-\theta)$$

$$\times \left\langle \frac{1}{2} s_3, lm \middle| \frac{1}{2} s_3' \right\rangle L_l(q), \qquad (2.9)$$

$$\langle {}^3\mathrm{H}, s_3' | j_\lambda(\mathbf{q}) | {}^3\mathrm{He}, s_3 \rangle = \sqrt{3\pi} \, i d_{m,-\lambda}^1(-\theta) \left\langle \frac{1}{2} s_3, lm \middle| \frac{1}{2} s_3' \right\rangle$$

$$\times [-\lambda M_1(q) + E_1(q)], \qquad (2.10)$$

where $m = s_3' - s_3$, $\lambda = \pm 1$, and C_l, L_l, E_l, and M_l denote the reduced matrix elements (RME's) of the Coulomb (C), longitudinal (L), transverse electric (E), and transverse magnetic (M) multipole operators, as defined in Refs. [20,22,23]. The $d_{m,m'}^l$ are rotation matrices in the standard notation of Ref. [25]. Since the weak charge and current operators have scalar/polar-vector (V) and pseudoscalar/axial-vector (A) components, each multipole consists of the sum of V and A terms, having opposite parity under space inversions [20]. Parity and angular-momentum selection rules restrict the contributing RME's to $C_0(V)$, $C_1(A)$, $L_0(V)$, $L_1(A)$, $E_1(A)$, and $M_1(V)$ in the ^{3}He$(\mu^-, \nu_\mu)^3$H process.

When the triton polarization is not detected, the differential capture rate for the reaction (1.1) is given by

$$d\Gamma = 2\pi \delta(m_\mu + m_\tau - E_\nu - \sqrt{m_t^2 + k_\nu^2}) |\bar{T}_W|^2 \frac{d\mathbf{k}_\nu}{(2\pi)^3}, \qquad (2.11)$$

where m_μ, m_τ, and m_t are the rest masses of the muon, ^{3}He, and ^{3}H, respectively, and the binding energy of the muonic atom has been neglected. Note that the following definition has been introduced:

$$|\bar{T}_W|^2 = \sum_{s_3', h_\nu} \sum_{f, f_z} P(f, f_z) |T_W(f, f_z; s_3', h_\nu)|^2, \qquad (2.12)$$

where $P(f, f_z)$ is the probability of finding the $\mu^- \, {}^3$He system in the total-spin state $|f f_z\rangle$. Integrating over the neutrino energy, the differential capture rate reduces to

$$\frac{d\Gamma}{d(\cos\theta)} = \frac{1}{2} \Gamma_0 \left[1 + A_v P_v \cos\theta + A_t P_t \left(\frac{3}{2} \cos^2\theta - \frac{1}{2} \right) \right.$$

$$\left. + A_\Delta P_\Delta \right], \qquad (2.13)$$

where the total capture rate Γ_0 reads

$$\Gamma_0 = G_V^2 E_\nu^2 \left(1 - \frac{E_\nu}{m_t} \right) |\psi_{1s}^{\mathrm{av}}|^2 \bar{\Gamma}_0, \qquad (2.14)$$

with $\bar{\Gamma}_0$ denoting the following combination of RME's:

$$\bar{\Gamma}_0 \equiv |C_0(V) - L_0(V)|^2 + |C_1(A) - L_1(A)|^2$$

$$+ |M_1(V) - E_1(A)|^2. \qquad (2.15)$$

The angular correlation parameters A_v, A_t, and A_Δ are given by

$$A_v = 1 + \frac{1}{\bar{\Gamma}_0} (2 \, \mathrm{Im}\{[C_0(V) - L_0(V)][C_1(A) - L_1(A)]^*\}$$

$$- |M_1(V) - E_1(A)|^2), \qquad (2.16)$$

$$A_t = \frac{4}{3} \frac{1}{\overline{\Gamma}_0} \left(\text{Im}\{[C_0(V) - L_0(V)][C_1(A) - L_1(A)]^*\} \right.$$

$$- \frac{1}{\sqrt{2}} \text{Im}\{[C_0(V) - L_0(V)][M_1(V) - E_1(A)]^*\}$$

$$+ \frac{1}{\sqrt{2}} \text{Re}\{[C_1(A) - L_1(A)][M_1(V) - E_1(A)]^*\}$$

$$\left. - \frac{1}{2} |M_1(V) - E_1(A)|^2 \right), \tag{2.17}$$

$$A_\Delta = \frac{2}{3} \frac{1}{\overline{\Gamma}_0} \left(\sqrt{2} \, \text{Im}\{[C_0(V) - L_0(V)][M_1(V) - E_1(A)]^*\} \right.$$

$$- \sqrt{2} \, \text{Re}\{[C_1(A) - L_1(A)][M_1(V) - E_1(A)]^*\}$$

$$+ \text{Im}\{[C_0(V) - L_0(V)][C_1(A) - L_1(A)]^*\}$$

$$\left. - \frac{1}{2} |M_1(V) - E_1(A)|^2 \right). \tag{2.18}$$

Finally, the coefficients P_v, P_t, and P_Δ are linear combinations of the probabilities $P(f, f_z)$, and are defined as [7,11]

$$P_v = P(1,1) - P(1,-1),$$

$$P_t = P(1,1) + P(1,-1) - 2P(1,0), \tag{2.19}$$

$$P_\Delta = P(1,1) + P(1,-1) + P(1,0) - 3P(0,0) = 1 - 4P(0,0).$$

Therefore P_v and P_t are proportional to the vector and tensor polarizations of the $f=1$ state, respectively, while P_Δ indicates the deviation of the $f=0$ population density from its statistical factor 1/4. Because of the small energy splitting between the $f=0$ and $f=1$ hyperfine states (1.5 eV) compared to the $\mu^- {}^3$He binding energy, and hence small deviation of $P(f, f_z)$ from its statistical value, direct measurements of the angular correlation parameters are rather difficult [1,8,11].

III. WEAK CHARGE AND CURRENT OPERATORS

An exhaustive description of the model for the nuclear weak current has been recently given in Ref. [20]. Here only its main features are summarized, and the new pseudoscalar contributions are discussed.

The nuclear weak current consists of vector and axial-vector parts, with corresponding one- and two-body components. The weak vector current is constructed from the isovector part of the electromagnetic current, in accordance with the conserved-vector-current (CVC) hypothesis. One important difference between the present calculations and those reported in Ref. [20] is that the leptonic four-momentum transfer is not negligible, but in fact close to the muon rest mass. Consequently, electromagnetic form factors need to be included in the expressions listed in Ref. [20]. The parametrization used for these reproduces available eN elas-

tic scattering data. Furthermore, in the present work the Darwin-Foldy relativistic correction to the vector charge operator is also included.

The one-body terms in the axial charge and current operators have the standard expressions [20] obtained from the nonrelativistic reduction of the covariant single-nucleon current, and include terms proportional to $1/m^2$, m being the nucleon mass. The induced pseudoscalar contributions are retained both in the axial current and charge operators. In particular, the pseudoscalar axial charge operator is taken as

$$\rho_{i,PS}^{(1)}(\mathbf{q};A) = -\frac{g_{PS}}{2mm_\mu}(m_\mu - E_\nu)(\boldsymbol{\sigma}_i \cdot \mathbf{q})\tau_{i,-}, \tag{3.1}$$

in the notation of Ref. [20].

Again, because the leptonic momentum transfer involved in muon capture is not negligible, axial and induced pseudoscalar form factors need to be included. These are parametrized as

$$g_A(q_\sigma^2) = \frac{g_A}{(1 + q_\sigma^2/\Lambda_A^2)^2}, \tag{3.2}$$

$$g_{PS}(q_\sigma^2) = -\frac{2m_\mu m}{m_\pi^2 + q_\sigma^2} g_A(q_\sigma^2), \tag{3.3}$$

where q_σ^2 is the four-momentum transfer. The axial-vector coupling constant g_A is taken to be [26] 1.2654 ± 0.0042, by averaging values obtained from the beta asymmetry in the decay of polarized neutrons and the half-lives of the neutron and superallowed $0^+ \rightarrow 0^+$ transitions. The value for the cut-off mass Λ_A is found to be approximately 1 GeV/c^2 from an analysis of pion electro-production data [27] and measurements of the reaction $p(\nu_\mu, \mu^+)n$ [28]. The q_σ^2 dependence of g_{PS} is obtained in accordance with the partially conserved-axial-current (PCAC) hypothesis, by assuming pion-pole dominance and the Goldberger-Treiman relation [21–23], m_π here indicates the pion mass.

Some of the two-body axial-current operators are derived from π- and ρ-meson exchanges and the $\rho\pi$-transition mechanism. These mesonic operators, first obtained in a systematic way in Ref. [29], give rather small contributions [20]. The two-body weak axial-charge operator includes a pion-range term, which follows from soft-pion theorem and current algebra arguments [30,31], and short-range terms, associated with scalar- and vector-meson exchanges. The latter are obtained consistently with the two-nucleon interaction model, following a procedure [32] similar to that used to derive the corresponding weak vector-current operators [20]. The two-body axial charge operator due to $N\Delta$ transition is also included [20], but its contribution is found to be very small.

The dominant two-body axial current operator is that due to Δ-isobar excitation [18,20]. We briefly review here its main features. The $N\Delta$-transition axial current is written as (notation as in Ref. [20])

TABLE I. Values for $R_A = g_A^*/g_A$, where g_A^* is the $N\Delta$ transition axial coupling constant (see, however, Sec. III for a discussion of the proper interpretation of g_A^*). The results are obtained by reproducing the experimental value of the Gamow-Teller (GT) matrix element in tritium β decay with CHH wave functions corresponding to the AV18, AV14, AV18/UIX, and AV14/TM Hamiltonian models. The theoretical uncertainties are due to the experimental error with which the GT matrix element is known.

Interaction model	g_A^*/g_A
AV18	1.25 ± 0.10
AV14	1.11 ± 0.09
AV18/UIX	1.17 ± 0.09
AV14/TM	1.04 ± 0.09

$$J_i^{(1)}(\mathbf{q}; N \to \Delta, A) = -\left[g_A^*(q_\sigma^2)\mathbf{S}_i \right.$$
$$\left. + \frac{g_{PS}^*(q_\sigma^2)}{2mm_\mu}\mathbf{q}(\mathbf{S}_i \cdot \mathbf{q}) \right] e^{i\mathbf{q}\cdot\mathbf{r}_i}T_{i,\pm},$$

(3.4)

where $\mathbf{S}_i$ and $\mathbf{T}_i$ are spin- and isospin-transition operators, which convert a nucleon into a Δ. The induced pseudoscalar contribution, ignored in Ref. [20], has been obtained from a nonrelativistic reduction of the covariant $N\Delta$-transition axial current [21].

The axial and pseudoscalar form factors g_A^* and g_{PS}^* are parametrized as

$$g_A^*(q_\sigma^2) = R_A g_A(q_\sigma^2),$$

(3.5)

$$g_{PS}^*(q_\sigma^2) = -\frac{2m_\mu m}{m_\pi^2 + q_\sigma^2}g_A^*(q_\sigma^2),$$

with $g_A(q_\sigma^2)$ given in Eq. (3.2). The parameter R_A is adjusted to reproduce the experimental value of the Gamow-Teller matrix element in tritium β decay, $\mathrm{GT}^{\mathrm{EXP}} = 0.957 \pm 0.003$ [18], while the q_σ^2 dependence of g_{PS}^* is again obtained by assuming pion-pole dominance and PCAC [21–23]. The values for R_A determined in the present study are listed in Table I for the four different combinations of interaction models. The experimental error on $\mathrm{GT}^{\mathrm{EXP}}$ is responsible for the 8–9% uncertainty in R_A.

Before concluding this section, a couple of remarks are in order. First, it is important to note that the value of R_A depends on how the Δ-isobar degrees of freedom are treated. In the present work, the two-body Δ-excitation operator is derived in the static Δ approximation, using first-order perturbation theory (see Ref. [20]). This approach is considerably simpler than that adopted in Ref. [20], where the Δ degrees of freedom were treated nonperturbatively, by retaining them explicitly in the nuclear wave functions [33]. The results for R_A obtained within the perturbative (PT) and nonperturbative (TCO) schemes differ by more than a factor of 2—see Table VI of Ref. [20]: $R_A(\mathrm{PT}) = 1.22$ and $R_A(\mathrm{TCO}) = 2.87$. [Note that the value for $R_A(\mathrm{PT})$ reported in Ref. [20] is slightly

TABLE II. Binding energies in MeV of ^{3}He and ^{3}H calculated with the CHH method using the AV18, AV14, AV18/UIX, and AV14/TM Hamiltonian models. Also listed are the experimental values.

Interaction model	^{3}He	^{3}H
AV18	6.917	7.617
AV14	7.032	7.683
AV18/UIX	7.741	8.473
AV14/TM	7.809	8.485
Expt.	7.72	8.48

different from that given here in Table I, since that value was obtained from a random walk consisting of 100 000 configurations, while the number of configurations sampled in the present work is 150 000.] However, the results for the observables calculated consistently within the two different schemes are typically within 1% of each other.

Second, because of the procedure adopted to determine R_A, the coupling constant $g_A^* = R_A g_A$ cannot be naively interpreted as the $N\Delta$ axial coupling constant. The excitation of additional resonances and their associated contributions will contaminate the value of g_A^*. Indeed, the PCAC arguments used above imply $g_A^*/g_A = f_{\pi N\Delta}/f_{\pi NN}$, where $f_{\pi NN}$ and $f_{\pi N\Delta}$ are the πNN and $\pi N\Delta$ coupling constants, and therefore one would obtain on the basis of Table I that $(f_{\pi N\Delta}/f_{\pi NN})^2$ is in the range 1.08–1.56, smaller than the value inferred from the Δ width, 4.67, and even smaller than the quark-model prediction, 2.88.

IV. RESULTS

In this section results for the ^{3}He$(\mu^-, \nu_\mu)^3$H capture process are reported. The trinucleon wave functions have been obtained from a realistic Hamiltonian consisting of the Argonne v_{18} (AV18) [16] two-nucleon and Urbana IX (UIX) [17] three-nucleon interactions. To compare with earlier predictions [11,12] for the same process, and to have some estimate of the model dependence, the older Argonne v_{14} (AV14) [13] two-nucleon and Tucson-Melbourne (TM) [14] three-nucleon interactions have also been used. Note that both the UIX and TM interactions have been adjusted to reproduce the triton binding energy. Finally, to investigate the effect of the three-nucleon interaction, predictions for muon-capture observables have been made by including only two-nucleon interactions (AV14 or AV18) in the Hamiltonian models.

The three-body bound-state problem has been solved with the correlated-hyperspherical-harmonics (CHH) method, as described in Refs. [34,35]. It consists essentially in expanding the wave function on the CHH basis, and in determining variationally the expansion coefficients by applying the Rayleigh-Ritz variational principle.

The ^{3}H and ^{3}He binding energies are listed in Table II for the different model Hamiltonians employed in the present work. They are obtained including only the isospin 1/2 com-

TABLE III. Capture rate Γ_0 in sec^{-1}, and angular correlation parameters A_v, A_t, and A_Δ, as defined in Eqs. (2.14)–(2.18), calculated using CHH wave functions corresponding to the AV18, AV14, AV18/UIX, and AV14/TM Hamiltonian models. The theoretical uncertainties, shown in parentheses, reflect the uncertainty in the determination of the $N\Delta$ transition axial coupling constant g_A^*.

Observable	AV18	AV14	AV18/UIX	AV14/TM
Γ_0	1441(7)	1444(7)	1484(8)	1486(8)
A_v	0.5341(14)	0.5339(14)	0.5350(14)	0.5336(14)
A_t	$-0.3642(9)$	$-0.3643(9)$	$-0.3650(9)$	$-0.3659(9)$
A_Δ	$-0.1017(16)$	$-0.1018(16)$	$-0.1000(16)$	$-0.1005(17)$

ponents of the wave functions. These results, which are very accurate (the uncertainty is of the order of one keV), are in excellent agreement with the values calculated using other techniques (for a review, see Ref. [36]).

Results for the capture rate Γ_0 and angular correlation parameters A_v, A_t, and A_Δ, defined in Eqs. (2.14)–(2.18), are presented in Table III. The uncertainty (in parentheses) in the predicted values is due to the uncertainty in the determination of the $N\Delta$ transition coupling constant g_A^* (see Sec. III and Table I). The latter reflects the experimental error in the Gamow-Teller matrix element of tritium β decay.

Inspection of Table III shows that the theoretical determination of the total capture rate Γ_0, when the AV18/UIX and AV14/TM Hamiltonian models are used, is within 1% of the recent experimental result [5], 1496 ± 4 sec^{-1}. When the theoretical and experimental uncertainties are taken into consideration, the agreement between theory and experiment is excellent. Furthermore, the model dependence in the calculated observables is very weak: the AV18/UIX and AV14/TM results differ by less than 0.5%. The agreement between theory and experiment and the weak model dependence mentioned above reflect, to a large extent, the fact that both the AV18/UIX and AV14/TM Hamiltonian models reproduce: (i) the experimental binding energies as well as the charge and magnetic radii [37] of the trinucleons; (ii) the Gamow-Teller matrix element in tritium β decay. In this respect, it is interesting to note that the capture rates predicted by the AV18 and AV14 Hamiltonian models are about 4% smaller than the experimental value, presumably because of the underprediction of the binding energies and consequent overprediction of

the radii. This makes the relevant nuclear form factors, entering into the expression for the rate Γ_0, smaller at the momentum transfer of interest, $q\simeq103$ MeV/c, than they would be otherwise. To study how the rate Γ_0 scales with the triton binding energy, we have repeated the calculation using CHH wave functions obtained with a modified AV14/TM Hamiltonian model, which gives for the ^{3}H and ^{3}He binding energies 9.042 and 8.349, respectively. The result for the rate Γ_0 is 1509 ± 7 sec^{-1}, while the angular correlation parameters are very close to the AV14/TM values listed in Table III. Therefore the rate Γ_0 scales approximately linearly with the trinucleon binding energy. The values for the angular correlation parameter A_v listed in Table III can be compared with the experimental result of Ref. [8], 0.63 ± 0.09 (stat.)$^{+0.11}_{-0.14}$ (syst.). Theory and experiment are in agreement, for any of the Hamiltonian models considered here. However, the experimental uncertainty is much larger than the theoretical one.

The contributions of the different components of the weak current and charge operators to the observables and to the RME's of the contributing multipoles are reported for the AV18/UIX model in Tables IV, and V–VI, respectively. The coupling constant g_A^* has been set equal to the central value of 1.17 g_A (see Table I). The notation in Tables IV, V, and VI is as follows. The column labeled "One-body no PS" lists the contributions associated with the one-body terms of the vector and axial charge and current operators, including relativistic corrections proportional to $1/m^2$. However, the induced pseudoscalar contributions are not considered in both

TABLE IV. Cumulative contributions to the capture rate Γ_0 (in sec^{-1}) and angular correlation parameters A_v, A_t, and A_Δ. The CHH wave functions are obtained using the AV18/UIX Hamiltonian model. The column labeled "One-body no PS" lists the contributions associated with the one-body vector and axial charge and current operators, but no induced pseudoscalar axial term is included. This is done in the column labeled "One-body," while the column labeled "Mesonic" lists the results obtained by including, in addition, the contributions from meson-exchange mechanisms. Finally the column labeled "Δ no PS" lists the results obtained by including also the Δ-excitation contributions, with g_A^*/g_A set to the central value of 1.17 (see Table I), but excluding the Δ pseudoscalar term, which is included in the column labeled "Full."

Observable	One-body no PS	One-body	Mesonic	Δ no PS	Full
Γ_0	1530	1316	1384	1493	1484
A_v	0.7735	0.5749	0.5511	0.5438	0.5350
A_t	-0.0840	-0.3565	-0.3679	-0.3525	-0.3650
A_Δ	-0.1424	-0.0686	-0.0810	-0.1038	-0.1000

TABLE V. Cumulative contributions to the reduced matrix elements (RME's) $C_0(V)$, $C_1(A)$, $L_1(A)$, $E_1(A)$, and $M_1(V)$. The CHH wave functions are obtained using the AV18/UIX Hamiltonian model. Note that $C_0(V)$ is purely real, while the other RME's are purely imaginary. Notations as in Table IV.

RME	One-body no PS	One-body	Mesonic	Δ no PS	Full
$C_0(V)$	0.3280		0.3277		
$C_1(A)$	-0.7532×10^{-2}	-0.4076×10^{-2}	-0.4135×10^{-2}	-0.4397×10^{-2}	
$L_1(A)$	0.4058	0.2590	0.2618	0.2804	0.2737
$E_1(A)$	0.5519		0.5563	0.5813	
$M_1(V)$	-0.1128		-0.1314	-0.1355	

the axial current and charge operators. Therefore the "One-body no PS" contribution is associated with the operators given in Eqs. (4.5)–(4.7), (4.8), (4.10), and (4.11)–(4.13) of Ref. [20], suitably modified by the inclusion of nucleon form factors, as explained in Sec. III. The column labeled "One-body" lists the contribution obtained when, in addition, the induced pseudoscalar axial charge and current operators, Eq. (3.1) and last term of Eq. (4.13) of Ref. [20], respectively, are also included.

The column labeled "Mesonic" lists the results obtained by including, in addition, the contributions from two-body vector and axial charge and current operators, associated with pion- and vector-meson exchanges, i.e., the πV and ρV for the vector current and charge operators, the πA, ρA, and $\rho\pi A$ for the axial current operator, and the πA, sA, and vA for the axial charge operator. We have used the notation of Ref. [20], where these terms are listed respectively in Eqs. (4.16)–(4.17), (4.30)–(4.31), (4.32)–(4.34), and (4.35)–(4.37). All these operators have been again modified by the inclusion of form factors.

The column labeled "Δ no PS" lists the contributions arising from Δ excitation, but does not include those due to the induced pseudoscalar Δ current of Eq. (3.4). The latter are retained in the column labeled "Full." The associated operators are obtained, as mentioned earlier in Sec. III, using perturbation theory and the static Δ approximation as in Eqs. (4.44), (4.48), (4.50), and (4.52) of Ref. [20].

Note that in Tables V and VI the values for the RME $L_0(V)$ have not been listed, since the charge and longitudinal multipole operators of the weak vector current, denoted respectively as $C_{ll_z}(q;V)$ and $L_{ll_z}(q;V)$, are related via CVC as [20]

$$L_{ll_z}(q;V) = -\frac{1}{q}[H,C_{ll_z}(q;V)]. \qquad (4.1)$$

In turn, this implies the following proportionality between the corresponding RME's $C_0(V)$ and $L_0(V)$, $L_0(V) = (m_\tau - m_t - q^2/2m_t)C_0(V)/q$, or $L_0(V) \simeq -0.024C_0(V)$ for $q \simeq 103$ MeV/c. Finally, in Table V the induced pseudoscalar axial contributions are present only in $C_1(A)$ and $L_1(A)$, but not in $E_1(A)$, since the pseudoscalar current is longitudinal.

The importance of the induced pseudoscalar contribution can be understood by inspection of Table IV. The nucleon induced pseudoscalar term in the axial current and charge operators reduce the value of Γ_0 by about 16%, while the

changes in the polarization observables are even larger. Far less important is the contribution from the pseudoscalar Δ current, which reduces the value of Γ_0 by less than 1%. The changes in the polarization observables are also small, a few %.

Among the observables, Γ_0 and A_Δ are the most sensitive to two-body contributions in the weak current. These are in fact crucial for reproducing the experimental capture rate, see Table IV. Inspection of Table V shows that two-body contributions are significant in the RME's $M_1(V)$, $L_1(A)$, and $E_1(A)$, but negligible in $C_0(V)$. The $C_0(V)$ and $M_1(V)$ RME's are related by CVC to the corresponding RME's of the isovector part of the electromagnetic current, since

$$\mathbf{j}_-(\mathbf{q};V) = [T_-,\mathbf{j}_{iv}(\mathbf{q};\gamma)], \qquad (4.2)$$

where $\mathbf{j}_-(\mathbf{q};V)$ is charge-lowering weak vector current, $\mathbf{j}_{iv}(\mathbf{q};\gamma)$ is the isovector part of the electromagnetic current, and T_- is the (total) isospin-lowering operator. A similar relation holds between the electromagnetic charge operator and its weak vector counterpart. Thus, if ^{3}He and ^{3}H were truly members of an isospin doublet, then the $C_0(V)$ and $M_1(V)$ RME's would just be proportional to the isovector combination of the trinucleon charge and magnetic form factors. Of course, electromagnetic terms and isospin-symmetry-breaking strong-interaction components in the nuclear potentials spoil this property. For example, the AV18/UIX model predicts for the isovector RME's $C_{0,iv}(\gamma)$ and $M_{1,iv}(\gamma)$ at $q \simeq 103$ MeV/c the values 0.3250 and -0.1385 (0.3254 and -0.1113 in impulse approximation), respectively.

The $C_1(A)$ RME is about two orders of magnitude smaller than the leading RME's, as expected on the basis of the following naive argument. The one-body axial charge density operator can be written approximately as (the notation is that of Ref. [20])

$$\rho_i^{(1)}(\mathbf{x};A) = -\frac{g_A}{2m}\tau_{i,-}\boldsymbol{\sigma}_i\cdot[\mathbf{p}_i,\delta(\mathbf{x}-\mathbf{r}_i)]_+$$

$$\simeq i\frac{g_A}{2m}\tau_{i,-}\boldsymbol{\sigma}_i\cdot\nabla_i\delta(\mathbf{x}-\mathbf{r}_i), \qquad (4.3)$$

where the term proportional to $\mathbf{p}_i$ has been neglected, and the identity $[A,B]_+ = [A,B]_- + 2BA$ has been used. Here $[A,B]_\pm$ denote the anticommutator (+) and commutator

TABLE VI. Individual mesonic contributions to the reduced matrix elements (RME's) $C_0(V)$, $C_1(A)$, $L_1(A)$, $E_1(A)$, and $M_1(V)$. The CHH wave functions are obtained using the AV18/UIX Hamiltonian model. Note that $C_0(V)$ is purely real, while the other RME's are purely imaginary. Notations as explained in the text.

RME	$\pi(V/A)$	$\rho(V/A)$	$\rho\pi A$	sA	vA
$C_0(V)$	-0.3285×10^{-3}	-0.6950×10^{-4}			
$C_1(A)$	-0.3253×10^{-5}			-0.2730×10^{-3}	0.2174×10^{-3}
$L_1(A)$	0.2324×10^{-2}	-0.2894×10^{-2}	0.3409×10^{-2}		
$E_1(A)$	0.2539×10^{-2}	-0.4208×10^{-2}	0.6056×10^{-2}		
$M_1(V)$	-0.1597×10^{-1}	-0.2627×10^{-2}			

($-$), respectively. We have also neglected the induced pseudoscalar contribution. The one-body axial current density (its leading term) is

$$\mathbf{j}_{i,\mathrm{NR}}^{(1)}(\mathbf{x};A)=-g_A\tau_{i,-}\boldsymbol{\sigma}_i\delta(\mathbf{x}-\mathbf{r}_i),\qquad(4.4)$$

and insertion of the approximation (4.3) and Eq. (4.4) into the expressions for the charge and longitudinal multipole operators leads to the following relation between the associated RME's: $C_1(A)\simeq-(q/2m)L_1(A)$, which, for $q\simeq103$ MeV/c, gives $C_1(A)\simeq-0.055L_1(A)$, i.e., the correct sign and order of magnitude obtained in the calculation.

Last, from inspection of Table VI, it is interesting to note that the contribution πA from the pion-exchange axial charge operator, which would be expected to be dominant among the two-body contributions to $C_1(A)$, is also negligible. In fact, the operator structure of the corresponding $C_1(A)$ multipole is such that it cannot connect the dominant S-wave components in the ^{3}He and ^{3}H wave functions, and the associated matrix element is therefore highly suppressed. Furthermore, the πA, ρA, and $\rho\pi A$ contributions to $L_1(A)$ and $E_1(A)$ are about two orders of magnitude smaller than the leading one-body term (see Table IV), and the relative signs of these contributions are such that they essentially cancel out in the total sum. This feature of the mesonic contributions to the axial current was already found in other low-energy weak processes [18–20].

In order to compare with the results of Ref. [11], the capture rate and angular correlation parameters have been calculated with the CHH wave functions corresponding to the AV14/TM Hamiltonian, and with a model for the nuclear weak current including only one-body terms. The values for the coupling constants and form factors entering the expressions for the charge and current operators have been taken from Ref. [11]. The comparison between the present and earlier predictions is shown in Table VII: there is satisfactory agreement between the two calculations. The remaining 1–3% differences can presumably be explained as follows: (i) the nuclear wave functions have been obtained with an AV14/TM Hamiltonian model with slightly different cutoff parameters [38]; (ii) the weak one-body operators in Ref. [11] include some of the next-to-next-to-leading orders in the nonrelativistic expansion of the covariant single-nucleon current, proportional to $1/m^3$; these are ignored in the present calculation; (iii) the numerical evaluation of the required matrix elements is performed with different techniques. Here,

Monte Carlo methods based on the Metropolis *et al.* algorithm [39] have been used. Typically, the statistical error on the calculated capture rate is less than 0.05%.

The results listed in Table III, column labeled "AV14/TM," are also in good agreement with those of Table IX of Ref. [12], although the treatment of the short-range behavior of the two-body terms in the weak current as well as the values for the vector and axial form factors, coupling constants, etc., in Ref. [12] are slightly different from those adopted in the present work. It is important to emphasize, though, that the present model for the weak current reproduces well the available experimental data: (i) the isovector component of the electromagnetic current, which by CVC is related to the weak vector current, leads to predictions for the isovector combination of the charge and magnetic form factors of ^{3}He and ^{3}H in excellent agreement with the measured values [37] up to momentum transfer of $\simeq3$ fm^{-1}; (ii) the two-body axial current operators are constrained to reproduce the Gamow-Teller matrix element in tritium β decay.

To test the sensitivity of all the muon capture observables to the induced pseudoscalar form factors g_{PS} and g_{PS}^*, Eqs. (3.3) and (3.5), we have repeated the calculation using AV18/UIX CHH wave functions and several different values of g_{PS} and g_{PS}^* in terms of their PCAC predictions g_{PS}^{PCAC} and $g_{PS}^{*\,\mathrm{PCAC}}$. We have assumed

$$R_{PS}\equiv\frac{g_{PS}}{g_{PS}^{\mathrm{PCAC}}}=\frac{g_{PS}^*}{g_{PS}^{*\,\mathrm{PCAC}}}.\qquad(4.5)$$

The variation of each observable in terms of R_{PS} is displayed in Fig. 1. The angular correlation parameters, in particular A_t and A_Δ, are more sensitive to changes in g_{PS} and

TABLE VII. Capture rate Γ_0 (in sec^{-1}) and angular correlation parameters A_v, A_t, and A_Δ obtained with AV14/TM CHH wave functions, and only one-body operators (column labeled "One-body") are compared with the results of Table III of Ref. [11].

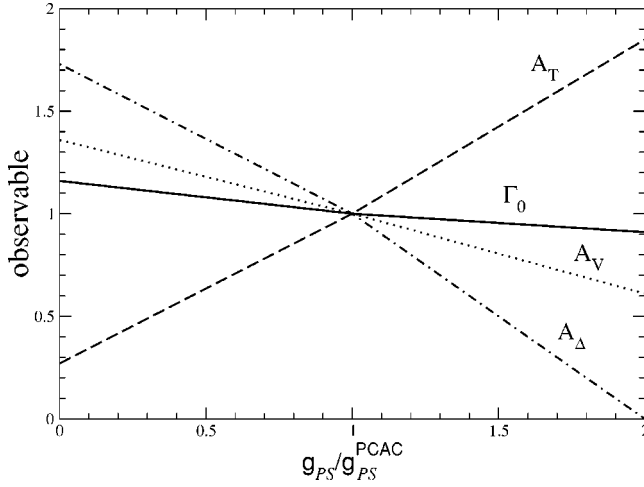| Observable	One-body	Ref. [11]
Γ_0	1287	1304
A_v	0.579	0.568
A_t	-0.351	-0.356
A_Δ	-0.070	-0.076

FIG. 1. Variation of the capture rate Γ_0 and angular correlation parameters A_v, A_t, and A_Δ with the induced pseudoscalar coupling g_{PS}. The AV18/UIX CHH wave functions are used. For each observable, the ratio between the result obtained with the given value of g_{PS} and the PCAC prediction, listed in Table III, is plotted versus the ratio g_{PS}/g_{PS}^{PCAC} ($=g_{PS}^*/g_{PS}^{*PCAC}$, see text).

g_{PS}^* than the total capture rate, as first pointed out in Ref. [7]. A precise measurement of these polarization observables could therefore be useful to ascertain the extent to which the induced pseudoscalar form factors deviate from their PCAC values.

Finally, by enforcing perfect agreement between the experimental and theoretical values, taken with their uncertainties, for the total capture rate Γ_0, it is possible to obtain an estimate for the range of values allowed for R_{PS}. The procedure adopted is the following: (i) we have considered the AV18/UIX minimum and maximum value for Γ_0 (see Table III), obtained with $R_{PS}=1$ and $R_A=1.08$ and 1.26, respectively (see Table I). (ii) For these two values of R_A, we have tuned R_{PS} to find Γ_0 within the experimental range. Our result for R_{PS} is then

$$R_{PS}=0.94\pm0.06. \tag{4.6}$$

This 6% uncertainty is smaller than that found in previous studies [11,12,40]. This substantial reduction in uncertainty can be traced back to the procedure used to constrain the (model-dependent) two-body axial currents described in Sec. III. In this respect, it is interesting to note that ignoring altogether the mesonic axial contributions associated with the π-, ρ-, and $\rho\pi$-exchange operators, and again re-adjusting the $N\Delta$ axial coupling constant to reproduce the tritium Gamow-Teller matrix element [in this case, $g_A^*=1.32(9)g_A$ is required] lead to the following predictions for the muon capture rate and angular correlation parameters: $\Gamma_0=1479(7)$ sec^{-1}, $A_v=0.5346(8)$, $A_t=-0.3666(14)$, and $A_\Delta=-0.0988(13)$. In this case, the extracted value for the ratio R_{PS} is 0.91 ± 0.06, in excellent agreement with the value of Eq. (4.6), suggesting that R_{PS} is not too sensitive to these mesonic contributions.

V. SUMMARY AND CONCLUSIONS

Muon capture observables for the process ^{3}He$(\mu^-,\nu_\mu)^3$H have been calculated with very accurate CHH wave functions corresponding to realistic Hamiltonians, the AV18/UIX and AV14/TM models, and with a nuclear weak current consisting of vector and axial-vector parts with one- and two-body terms. The conserved-vector-current hypothesis has been used to derive the weak vector charge and current operators from the isovector electromagnetic counterparts, while the axial current has been constructed to reproduce the measured Gamow-Teller matrix element of ^{3}H β decay. The axial current also includes the nucleon and Δ induced pseudoscalar current operators. It should be emphasized that the model adopted for the electromagnetic current provides an excellent description of the ^{3}He and ^{3}H charge and magnetic form factors [37] at low and medium values of momentum transfers.

The predicted total capture rate is in agreement with the experimental value, and has been found to have only a weak model dependence: the AV18/UIX and AV14/TM results differ by less than 0.5%. The weak model dependence can be traced back to the fact that both Hamiltonians reproduce the binding energies, charge, and magnetic radii of the trinucleons, and the Gamow-Teller matrix element in tritium β decay.

It is important to note that, if the contributions associated with two-body terms in the axial current were to be neglected, the predicted capture rate would be 1316 (1318) sec^{-1} with AV18/UIX (AV14/TM), and so two-body mechanisms are crucial for reproducing the experimental value. The present work demonstrates that the procedure adopted for constraining these two-body contributions leads to a consistent description of available experimental data on weak transitions in the three-body systems. It also corroborates the robustness of our recent predictions for the cross sections of the proton weak captures on ^{1}H [18] and ^{3}He [19,20], which were obtained with the same model for the nuclear weak current.

Finally, it would be interesting to study the ^{3}He$(\mu^-,\nu_\mu)nd$ and ^{3}He$(\mu^-,\nu_\mu)nnp$ processes, both of which have been investigated experimentally in Ref. [41] and theoretically in Ref. [42]. Since the CHH method is suitable to solve for the three-body bound and scattering states [43], the study of these two processes is also possible. Work along these lines is vigorously being pursued.

[1] D. F. Measday, Phys. Rep. **354**, 243 (2001).

[2] I. V. Folomkin *et al.*, Phys. Lett. **3**, 229 (1963).

[3] L. B. Auerbach *et al.*, Phys. Rev. **138**, B127 (1965).

[4] D. R. Clay, J. W. Keuffel, R. L. Wagner, and R. M. Edelstein, Phys. Rev. **140**, B587 (1965).

[5] P. Ackerbauer *et al.*, Phys. Lett. B **417**, 224 (1998).

[6] C. W. Kim and H. Primakoff, Phys. Rev. **140**, B566 (1965).

[7] W.-Y. P. Hwang, Phys. Rev. C **17**, 1799 (1978).

[8] P. A. Souder *et al.*, Nucl. Instrum. Methods Phys. Res. A **402**, 311 (1998).

[9] E. M. Peterson, Phys. Rev. **167**, 971 (1968).

[10] A. C. Phillips, F. Roig, and J. Ros, Nucl. Phys. **A237**, 493 (1974).

[11] J. G. Congleton and H. W. Fearing, Nucl. Phys. **A552**, 534 (1992).

[12] J. G. Congleton and E. Truhlìk, Phys. Rev. C **53**, 956 (1996).

[13] R. B. Wiringa, R. A. Smith, and T. A. Ainsworth, Phys. Rev. C **29**, 1207 (1984).

[14] S. A. Coon *et al.*, Nucl. Phys. **A317**, 242 (1979).

[15] H. Kameyama, M. Kamimura, and Y. Fukushima, Phys. Rev. C **40**, 974 (1989); M. Kamimura and H. Kameyama, Nucl. Phys. **A508**, 17c (1990).

[16] R. B. Wiringa, V. G. J. Stoks, and R. Schiavilla, Phys. Rev. C **51**, 38 (1995).

[17] B. S. Pudliner, V. R. Pandharipande, J. Carlson, and R. B. Wiringa, Phys. Rev. Lett. **74**, 4396 (1995).

[18] R. Schiavilla *et al.*, Phys. Rev. C **58**, 1263 (1998).

[19] L. E. Marcucci, R. Schiavilla, M. Viviani, A. Kievsky, and S. Rosati, Phys. Rev. Lett. **84**, 5959 (2000).

[20] L. E. Marcucci *et al.*, Phys. Rev. C **63**, 015801 (2001).

[21] T. R. Hemmert, B. R. Holstein, and N. C. Mukhopadhyay, Phys. Rev. D **51**, 158 (1995).

[22] J. D. Walecka, in *Muon Physics; Weak Interactions*, edited by V. W. Hughes and C. S. Wu (Academic, New York, 1975), p. 114.

[23] J. D. Walecka, *Theoretical Nuclear and Subnuclear Physics* (Oxford University Press, New York, 1995).

[24] J. C. Hardy, I. S. Towner, V. T. Koslowsky, E. Hagberg, and H. Schmeing, Nucl. Phys. **A509**, 429 (1990).

[25] A. R. Edmonds, *Angular Momentum in Quantum Mechanics* (Princeton University Press, Princeton, 1957).

[26] E. Adelberger *et al.*, Rev. Mod. Phys. **70**, 1265 (1998).

[27] E. Amaldi, S. Fubini, and G. Furlan, Electroproduction at Low Energy and Hadron Form Factors, Springer Tracts in Modern Physics No. 83, 1979, p. 1.

[28] T. Kitagaki *et al.*, Phys. Rev. D **28**, 436 (1983).

[29] M. Chemtob and M. Rho, Nucl. Phys. **A163**, 1 (1971).

[30] K. Kubodera, J. Delorme, and M. Rho, Phys. Rev. Lett. **40**, 755 (1978).

[31] I. S. Towner, Nucl. Phys. **A542**, 631 (1992).

[32] M. Kirchbach, D. O. Riska, and K. Tsushima, Nucl. Phys. **A542**, 616 (1992).

[33] R. Schiavilla, R. B. Wiringa, V. R. Pandharipande, and J. Carlson, Phys. Rev. C **45**, 2628 (1992).

[34] A. Kievsky, M. Viviani, and S. Rosati, Nucl. Phys. **A551**, 241 (1993).

[35] A. Kievsky, M. Viviani, and S. Rosati, Nucl. Phys. **A577**, 511 (1994).

[36] J. Carlson and R. Schiavilla, Rev. Mod. Phys. **70**, 743 (1998).

[37] L. E. Marcucci, D. O. Riska, and R. Schiavilla, Phys. Rev. C **58**, 3069 (1998).

[38] M. Kamimura (private communication).

[39] N. Metropolis *et al.*, J. Chem. Phys. **21**, 1087 (1953).

[40] J. Govaerts and J.-L. Lucio-Martinez, Nucl. Phys. **A678**, 110 (2000).

[41] S. E. Kuhn *et al.*, Phys. Rev. C **50**, 1771 (1994).

[42] R. Skibinski, J. Golak, H. Witala, and W. Glöckle, Phys. Rev. C **59**, 2384 (1999).

[43] A. Kievsky *et al.*, Phys. Rev. C **58**, 3085 (1998).